This document was prepared in conjunction with work accomplished under Contract No. DE-AC09-96SR18500 with the U. S. Department of Energy.

DISCLAIMER

WSRC-MS-2006-00167

An Unsteady Dual Porosity Representation Of Concrete Rubble Disposal

by

GREGORY FLACH

Westinghouse Savannah River Company
Savannah River Site
Aiken, South Carolina 29808

Additional Authors:

DOE Contract No. **DE-AC09-96SR18500**

An Unsteady Dual Porosity Representation of Concrete Rubble Disposal

G. P. Flach[1]*, K. P. Crapse[2], M. A. Phifer[1], L. B. Collard[2], and L. D. Koffman[1]

Decontamination and decommissioning at the Savannah River Site have produced on-site disposals of low-level solid radioactive waste in the form of concrete rubble. In the case of a former tritium extraction facility, building demolition produced a significant volume of rubble embedded with tritium. The contaminated debris comprises a heterogeneous mixture of sizes, shapes, and internal tritium distributions. The rubble was disposed in long, shallow, unlined, earthen trenches, that were subsequently backfilled with excavated soil and exposed to normal infiltration. To forecast tritium flux to the water table, an unsteady dual porosity model was developed to describe vadose zone leaching and transport. Tritium was assumed to be released through unsteady, one-dimensional, molecular diffusion within concrete, while advective and diffusive transport occur in the surrounding backfill. Rubble size and shape variations were characterized through a combination of physical measurement and photographic image analysis. For simplicity, the characterization data were reduced to an approximately equivalent distribution of one-dimensional slab thicknesses for representation in the dual porosity formulation. Each size classification was simulated separately, and individual flux results were then blended in proportion to the thickness distribution to produce a composite flux. The fractional flux from concrete rubble was predicted to be roughly 40% of that from tritium-contaminated soil. The lower flux is a result of slower release to soil pore water, and a reduced effective trench conductivity from the presence of impervious concrete.

[1] Savannah River National Laboratory, Savannah River Site, 773-42A, Aiken, SC 29808

[2] Savannah River National Laboratory, Savannah River Site, 773-43A, Aiken, SC 29808

* corresponding author (gregory.flach@srnl.doe.gov)

Introduction

Nuclear facility decontamination and decommissioning (D&D) activity at the Savannah River Site has produced on-site disposals of low-level solid radioactive waste in the form of concrete rubble. In the case of a former tritium extraction facility, Building 232-F demolition (Figure 1a) produced a significant volume of rubble with embedded tritium as HTO. Tritium (H-3) is non-sorbing in this form and decays with a half-life of 12.3 years. The contaminated concrete debris comprises a heterogeneous mixture of sizes, shapes, and internal tritium distributions (Figure 1b). The rubble was disposed in long, shallow, unlined, earthen trenches, that were subsequently backfilled with excavated soil and exposed to normal rainfall infiltration. An accurate prediction of tritium flux to the water table was desired in order to demonstrate compliance with U. S. Department of Energy performance objectives for on-site disposal. To this end, an unsteady dual porosity model was developed to describe concrete leaching and vadose zone transport.

The dual-porosity concept has been applied to several physical settings, including fractured media, laboratory soil columns, heterogeneous granular aquifers, and in the situation most analogous to the present, aggregated media (Passioura, 1971; Skopp and Warrick, 1974; van Genuchten and Wierenga, 1976, 1977; van Genuchten and others, 1977; Rao et al., 1980; Lafolie and Hayot, 1993a, b; Brusseau et al., 1994; Griffioen et al., 1998). Specific formulations range from “mobile-immobile” regions with first-order mass

transfer (Coats and Smith, 1964) to “dual-permeability” in which advection occurs in both regions (Gerke and van Genuchten, 1993). A number of generalizations have been developed (e.g. Haggerty and Gorelick, 1995; Wang et al. 2005a).

For the present application, the low permeability of intact concrete precludes significant advective transport, but an accurate representation of diffusive leaching from concrete was desired. Thus the “unsteady” dual-porosity model, in the terminology of Birkholzer and Rouve (1994), was chosen. The unsteady formulation incorporates Fick’s Second Law (Rasmuson and Neretnieks, 1980; Grisak and Pickens, 1980; Bibby, 1981; Huyakorn et al., 1983; van Genuchten, 1985), in contrast to first-order approaches. The unsteady dual-porosity model also avoids ambiguity (Griffioen et al., 1998) in the proper mass transfer coefficient setting for the simpler first-order approach, and readily accommodates non-uniform initial conditions.

The size and shape of concrete chunks have a strong effect on the rate of tritium leaching from building rubble. Leaching is relatively slow from large chunks with a low surface area to volume ratio. Small concrete pieces and/or a high surface area to volume ratio produce a fast release. Rather than explicitly consider every potential geometry in a leaching model, concrete rubble was approximated by a distribution of equivalent one-dimensional slabs in our approach. The size and shape variations of rubble were characterized through a combination of physical measurement and photographic image analysis. Each size classification was simulated separately to show the effect on flux. The individual flux results were then blended in proportion to the thickness distribution to produce a composite flux.

The following sections describe development of an unsteady dual-porosity model, an approach for approximating an arbitrary shape with a one-dimensional slab, characterization of concrete rubble, the influence of relatively impervious rubble on vadose zone flow, fractional flux as a function of characteristic size, and representative results in comparison to tritium-contaminated soil disposals.

Unsteady Dual-Porosity Model

Under humid Southeast U.S. conditions, buried concrete is assumed to be fully saturated for practical purposes. Liquid-phase molecular diffusion is considered to be the primary mechanism for tritium release to surrounding backfilled soil. The effective diffusion coefficient for tritium in concrete is estimated to be $5\times10^{-8}\,\mathrm{cm}^2/\mathrm{s}$, compared to about $5\times10^{-6}\,\mathrm{cm}^2/\mathrm{s}$ for soil. Therefore concentration gradients in the backfill can be neglected compared to those in concrete, and the boundary condition for diffusion in concrete is effectively the backfill tritium concentration. The mathematical formulation assumed for diffusive release from a one-dimensional slab of dimension s is

$$\begin{aligned} \frac{\partial C}{\partial t} &= D\frac{\partial^2 C}{\partial x^2} - \lambda C \\ C(0,t) = C(s,t) &= C_b(t) \\ C(x,0) &= C_0(x) \end{aligned} \qquad (1)$$

where concentration is denoted by C, D is the effective diffusion coefficient for porous medium transport, λ is the first-order coefficient for radioactive decay, and $C_0(x)$ is the initial concentration. After time zero, concentration at the two exterior surfaces varies with time according to $C_b(t)$, the tritium concentration in the backfill pore water. The flux leaving concrete rubble is computed as

$$F_b(t) = n_c D \left.\frac{\partial C}{\partial x}\right|_{x=0} - n_c D \left.\frac{\partial C}{\partial x}\right|_{x=s} \quad (2)$$

where n_c is the porosity of concrete.

For the backfilled soil residing between solid pieces of concrete, tritium is assumed to be transported by liquid-phase advection and dispersion. The standard advection-dispersion mathematical formulation is used. The concrete model is coupled to the backfill model through the concentration transient $C_b(t)$. The backfill model is coupled to the concrete model through the flux term $F_b(t)$. The overall coupled model is solved iteratively by alternating between concrete and backfill simulations and updating the concentration transients using an under-relaxation technique. The coupling approach is numerically inefficient, but simple and effective nonetheless.

Equivalent One-Dimensional Slab Thickness

One method for defining the thickness of an equivalent one-dimensional slab is to preserve the volume (V) and surface area (A) of the three-dimensional object (Figure 2). The resulting slab thickness (s) is

$$s = \frac{V}{A_f} = \frac{2V}{A} \quad (3)$$

where $A_f = A/2$ is the face area of the slab. The effectiveness of this approach can be assessed by comparing exact solutions for mass diffusion from a three-dimensional brick geometry and a one-dimensional slab of characteristic dimension defined by equation (3). The following initial value formulation is considered for simplicity:

$$\frac{\partial C}{\partial t} = D\left[\frac{\partial^2 C}{\partial x^2} + \frac{\partial^2 C}{\partial y^2} + \frac{\partial^2 C}{\partial z^2}\right]$$
$$C(0,y,z,t) = C(a,y,z,t) = 0$$
$$C(x,0,z,t) = C(x,b,z,t) = 0 \qquad (4)$$
$$C(x,y,0,t) = C(x,y,c,t) = 0$$
$$C(x,y,z,0) = C_0$$

The equation set describes diffusion from a brick with dimensions a,b,c and a uniform initial concentration of C_0. Concentration is denoted by C, and D is the effective diffusion coefficient for porous medium transport. After time zero, the exterior surfaces are held at a concentration of zero. First-order decay is omitted from equations (4) in order to focus solely on the impact of geometry (1D versus 3D) on diffusion. The exact series solution is (cf. Ozisik 1980)

$$C(x,y,z,t)/C_0 = \frac{64}{abc}\sum_{m=1}^{\infty}\sum_{n=1}^{\infty}\sum_{p=1}^{\infty}\frac{\exp(-D\beta_m^2 t)\exp(-D\gamma_n^2 t)\exp(-D\eta_p^2 t)}{\beta_m\gamma_n\eta_p} \cdot \sin(\beta_m x)\sin(\gamma_n y)\sin(\eta_p, z) \qquad (5)$$

with the eigenvalues defined as the positive roots of $\sin(\beta_m a) = \sin(\gamma_n b) = \sin(\eta_p c) = 0$.

For a brick with dimensions a,b,c equation (3) defining equivalent 1D slab thickness evaluates as

$$s = \frac{abc}{ab + bc + ac} \qquad (6)$$

and the exact series solution for a one-dimensional slab is

$$C(x,t)/C_0 = \frac{4}{s}\sum_{m=1}^{\infty}\frac{\exp(-D\beta_m^2 t)}{\beta_m} \cdot \sin(\beta_m x) \qquad (7)$$

with eigenvalues defined by $\sin(\beta_m s) = 0$.

The fraction of initial mass residing in the three-dimensional brick at time t can be derived by integrating equation (5) over the volume, with the result:

$$M_{3D}(t) = \int_0^a \int_0^b \int_0^c C(x,y,z,t)/C_0 \cdot dxdydz = \frac{512}{abc} \sum_{m=1}^{\infty} \sum_{n=1}^{\infty} \sum_{p=1}^{\infty} \frac{\exp(-D\beta_m^2 t)\exp(-D\gamma_n^2 t)\exp(-D\eta_p^2 t)}{\beta_m^2 \gamma_n^2 \eta_p^2} \quad (8)$$

Similarly, the mass fraction remaining in the one-dimensional slab is

$$M_{1D}(t) = \int_0^s C(x,t)/C_0 \cdot dx = \frac{8}{s} \sum_{m=1}^{\infty} \frac{\exp(-D\beta_m^2 t)}{\beta_m^2} \quad (9)$$

Figure 3 displays the relative residual mass curves for a block of unit dimensions ($1 \times 1 \times 1$ unitless) and a diffusion coefficient of one (non-dimensional parameter case), and the corresponding one-dimensional slab. For early times the two solutions agree exactly, because the primary control on flux is surface area. At later times, as the diffusion front penetrates the two geometries, shape also affects the flux. Cumulative flux from the one-dimensional slab is significantly larger compared to the three-dimensional block. As the three-dimensional block is flattened while holding volume constant, the agreement becomes better, as indicated by the example results for a brick of dimensions $1/4 \times 2 \times 2$, also shown in Figure 3.

Improved agreement between the 3D and 1D simulations can be achieved by empirically adjusting the thickness of the 1D slab while holding volume constant. Results such as those depicted in Figure 3 indicate that the more “three-dimensional” the shape from a

diffusion perspective, the less accurate the approximating one-dimensional slab. One measure of the "three-dimensional" nature of an object is the volume to surface area ratio. For a rectangular geometry, the ratio is maximized when the three sides are equal, i.e., the brick is a cube. Similarly for elliptical shapes, the surface area is minimized for the special case of a sphere. These special cases produce the maximum value of s in equation (3) for a fixed volume, as can be seen by noting that $V/A = s/2$. For both a cube and sphere

$$s = \frac{d}{3} \equiv s_{\max} \tag{10}$$

where d is either the side length for the cube or the diameter of the sphere, and is the largest possible value for a fixed volume. For a cube

$$d = V^{1/3} \tag{11}$$

and for a sphere

$$d = \left(\frac{6V}{\pi}\right)^{1/3} \tag{12}$$

For an arbitrary 3D shape, the ratio $s/s_{\max}$ is an indication of the three-dimensional nature of the object, and ranges between 0 and 1. An empirical adjustment factor to s, producing significantly improved agreement between the 1D and 3D results, is given by

$$f = 1 + (\sqrt{2} - 1)(s/s_{\max})^2 \tag{13}$$

and plotted in Figure 4. The revised slab thickness becomes

$$s_{rev} = fs \tag{14}$$

The empirical factor f was developed in this study by fitting the chosen functional form to calibration data. The calibration data consisted of optimal multipliers for a range of $s/s_{\max}$ values. The "round" numerical values in equation (13) have no particular theoretical basis, and other functional forms could be chosen to accomplish the same effect. Figure 5 compares the 1D and 3D results based on revised slab dimension. In addition to the $1\times1\times1$ and $1/4\times2\times2$ brick dimensions, results for a brick of dimensions $1/2\times\sqrt{2}\times\sqrt{2}$ are shown. The agreement is observed to be much improved, and adequate for the purpose of this study.

Concrete Rubble Size Distribution

The size and shape variations of concrete rubble from Building 232-F were estimated from comparable building demolition sites, through a combination of physical measurement and photographic image analysis. For each concrete chunk analyzed, an approximately equivalent one-dimensional slab thickness was derived from equations (3) and (10) through (14) from measurements of volume V and surface area A. Size distributions were defined in terms of a geometric series of discrete characteristic dimensions (Table 1), by grouping thicknesses within certain size ranges. Table 1 shows the estimated size distribution of rubble from 232-F demolition.

An example of photographic image analysis to determine V and A is depicted in Figure 6. The raw photograph (Figure 6a) was first translated into a two-dimensional map of larger individual chunks of concrete, clusters of smaller pieces, and void/air space, using Geographic Information System (GIS) software (Figure 6b). The 2D area and perimeter

of each polygon representing an individual concrete piece were computed by the GIS software. An approximating ellipse with the same area and perimeter as the polygon was then generated, followed by a 3D ellipsoid assuming that the third axis was the average of the two ellipse axes. Finally, the three axes were used to compute three-dimensional volume and surface area for the approximating ellipsoid.

Vadose Zone Flow and Transport

Concrete rubble in disposal trenches hinders release of embedded tritium, in comparison to tritium contaminated soil, thus reducing flux to the water table. Impervious concrete also impacts vadose zone flow within and surrounding the trench by lowering the effective vertical hydraulic conductivity of the composite trench. To the extent travel time from the trench to the water table increases, the flux of a relatively fast decaying nuclide such as tritium decreases. However, concrete also reduces the effective porosity for advective transport through backfilled soil, which increases pore velocities in the trench relative to Darcy velocities. The two phenomena compete, and the net effect is not obvious.

The volume of concrete in Building 232-F has been estimated at 1031 m^3, and disposal records indicate that about 1584 m^3 of rubble was buried in trenches. The volume increase is presumed to reflect bulking of the material. The data imply a volume fraction of solid concrete within bulked rubble of 65%. This percentage is consistent with the bulk density of shale rip-rap (105 lb/ft^3) and the rock density of shale (175 lb/ft^3), which imply an solid fraction of 60% for the bulked material. Disposal operations personnel estimated that 80-85% of the trench volume would typically be filled with rubble. Thus, the overall

fraction of solid concrete within the waste zone is estimated to be 0.825 × 0.65 = 0.54. Backfilled soil is assumed to occupy the remaining fraction of 0.46, after some initial settling. Soil backfill alone is estimated to have a porosity of 0.456 and hydraulic conductivity of 2×10^{-4} cm/s. Assuming a tortuosity of 2 for macroscopic flow around chunks of concrete, the porosity and conductivity of backfilled rubble are approximately $0.46\times0.456=0.21$ and $(0.46/2)\times(2\times10^{-4})=4.6\times10^{-5}$ cm/s respectively. The tortuosity value is based on the data of Wang et al. (2005b), who measured tortuosity for rock samples in the size range of 3.8 to 4.5 cm in diameter and 8.9 to 10.5 cm in length. Soil characteristic curves for backfilled soil are assumed to be unaltered by surrounding rubble.

Numerical Simulations

Nominal dimensions for the disposal trenches are 6.1 m (20 ft) wide and 6.1 m (20 ft) deep. Buried waste occupies the bottom 4.9 m (16 ft). The water table averages 14 m (45 ft) below grade, or 7.6 m below trench bottom. Annual average infiltration at the disposal facility is estimated to be 30 cm/yr from the HELP model simulations of infiltration (USEPA, 1994a, b). Trenches backfilled with soil (Figure 7a), and a combination of soil and concrete rubble (Figure 7b), were simulated. The simulated pathlines include one year time markers based on pore velocity. Note that impervious rubble increases pore velocity and reduces travel time through the trench, but reduces Darcy velocity and diverts moisture around the trench. The result of the latter two effects is slightly longer travel time between the trench and water table.

Figure 8 illustrates fractional flux (Ci/yr per Ci disposed) leaving the bottom of the burial trench as a function of characteristic thickness, and two initial distributions. For the non-uniform distribution, the initial activity is confined to a depth of 7.6 cm (3 inches) on one side of the slab, which Building 232-F characterization indicated to be representative of the stack (Figure 1a). The fractional flux curves for the non-uniform loading are observed to be quite similar, despite differing slab thickness. Figures 9 and 10 show how tritium flux and concentration vary with elevation in the trench, for rubble with an 8 cm characteristic dimension. Note that backfill concentration increases with depth (Figure 10) as tritium is carried downward from higher layers, thus reducing the early tritium release with depth (Figure 9). At later times, the bottom layers release tritium at a slightly higher rate than upper layers. Figure 11 illustrates fractional flux to the water table for tritium-contaminated soil only in the trench (instantaneous release), and concrete rubble with each of the characteristic dimensions defined in Table 1 plus a 0 cm asymptote. The latter is generated by assuming local equilibrium between the backfill and concrete concentrations.

The contaminated soil and 0 cm asymptote curves differ solely from the impact of impervious concrete on vadose zone flow (Figure 7), as both scenarios involves instantaneous release of tritium to mobile water. Peak flux declines with increasing concrete thickness. For the size distribution define in Table 1, a composite fractional flux curve for Building 232-F rubble was generated by blending the type curves shown in Figure 11. The resulting peak flux is approximately 40% of that for contaminated soil alone is a trench.

Summary

Concrete rubble disposal in earthen trenches at the Savannah River Site presents a unique opportunity to apply the unsteady dual-porosity transport formulation in an unconventional setting. The contaminated concrete debris comprises a heterogeneous mixture of sizes, shapes, and internal tritium distributions. Approximating the waste with a distribution of equivalent one-dimensional slab thicknesses is effective in capturing diffusional flux variations with concrete chuck size, shape and internal source distribution. The unsteady dual-porosity formulation facilitated more accurate forecast of tritium releases from burial trenches in comparison to prior assumptions of instantaneous release. Specifically, the peak fractional flux from concrete rubble is predicted to be roughly 40% of that from tritium-contaminated soil. The lower flux is a result of slower release of tritium from concrete, and a reduced effective hydraulic conductivity of the trench due to the presence of impervious concrete.

Acknowledgments

We are sincerely grateful to Washington Savannah River Company LLC and the U.S. Department of Energy for making this work possible under Contract No. DE-AC09-96SR18500 and for permission to publish our findings.

References

Bibby, R. 1981. Mass transport of solutes in dual-porosity media. Water Resources Research 17:1075-1081.

Birkholzer, J. and G. Rouve. 1994. Dual-continuum modeling of contaminant transport in fractured formations. In A. Peters et al. (eds.), Computational methods in water resources X:659-666. Kluwer Academic Publishers, Netherlands.

Brusseau, M. L., Z. Gerstl, D. Augustijn and P. S. C. Rao. 1994. Simulating solute transport in an aggregated soil with the dual-porosity model: Measured and optimized parameter values. Journal of Hydrology 163:187-193.

Coats, K. H. and B. D. Smith. 1964, Dead-end pore volume and dispersion in porous media, Society of Petroleum Engineers Journal, v 4, 73-84.

Gerke, H. H. and M. T. van Genuchten. 1993. A dual-porosity model for simulating the preferential movement of water and solutes in structured porous media. Water Resources Research 29:305-319.

Griffioen, J. W., D. A. Barry and J.-Y. Parlange. 1998. Interpretation of two-region model parameters. Water Resources Research 34:373-384.

Grisak, G. E. and J. F. Pickens. 1980. Solute transport through fractured media; 1. The effect of matrix diffusion. Water Resources Research 16:719-730.

Haggerty, R. and S. M. Gorelick. 1995. Multiple-rate mass transfer for modeling diffusion and surface reactions in media with pore-scale heterogeneity. Water Resources Research 31:2383-2400.

Huyakorn, P. S., B. H. Lester and J. W. Mercer. 1983. An efficient finite element technique for modeling transport in fractured porous media; 1. Single species transport. Water Resources Research 19:841-854.

Lafolie, F. and Ch. Hayot. 1993a. One-dimensional solute transport modelling in aggregated porous media . Part 1. Model description and numerical solution. Journal of Hydrology 143:63-83.

Lafolie, F. and Ch. Hayot. 1993b. One-dimensional solute transport modelling in aggregated porous media . Part 2. Effects of aggregate size distribution. Journal of Hydrology 143:85-107.

Ozisik, M. N. 1980. Heat conduction. John Wiley & Sons, New York.

Passioura, J. B. 1971. Hydrodynamic dispersion in aggregated media; I. Theory. Soil Science 111:339-344.

Rao, P. S. C., D. E. Rolston, R. E. Jessup and J. M. Davidson. 1980. Solute transport in aggregated porous media: Theoretical and experimental evaluation. Soil Science Society of America Journal 44:1139-1146.

Rasmuson A. and I. Neretnieks. 1980. Exact solution of a model for diffusion in particles and longitudinal dispersion in packed beds. A.I.Ch.E. Journal 26:686-690.

Skopp, J. and A. W. Warrick. 1974. A two-phase model for the miscible displacement of reactive solutes in soils. Soil Science Society of America Journal 38:545-550.

USEPA. 1994a. The Hydrologic Evaluation of Landfill Performance (HELP) model user's guide for version 3. EPA/600/R-94/168a. Office of Research and Development, United States Environmental Protection Agency, Washington, DC.

USEPA. 1994b. The Hydrologic Evaluation of Landfill Performance (HELP) engineering documentation for version 3. EPA/600/R-94/168b. Office of Research and Development, United States Environmental Protection Agency, Washington, DC.

van Genuchten M.Th. 1985. A general approach for modelling solute transport in structured soils. Int. Assoc. Hydrogeologists Memoires 17:513-526.

van Genuchten, M. T. and P. J. Wierenga. 1976. Mass transfer studies in sorbing porous media I. Analytical solutions. Soil Science Society of America Journal 40:473-480.

van Genuchten, M. T. and P. J. Wierenga. 1977. Mass transfer studies in sorbing porous media: II. Experimental evaluation with tritium (3H2O). Soil Science Society of America Journal 41:272-278.

van Genuchten, M. T., P. J. Wierenga and G. A. O'Connor. 1977. Mass transfer studies in sorbing porous media: III. Experimental evaluation with 2,4,5-T. Soil Science Society of America Journal 41:278-285.

Wang, P. P., C. Zheng and S. M. Gorelick. 2005a. A general approach to advective-dispersive transport with multirate mass transfer. Advances in Water Resources 28:33-42.

Wang, R., T. Pavlin, M. S. Rosen, R. W. Mair, D. G. Cory and R. L. Walsworth. 2005b. Xenon NMR measurements of permeability and tortuosity in reservoir rocks. Magnetic Resonance Imaging 23:329-331.

Tables

Table 1 Characteristic one-dimensional slab thicknesses simulated by the unsteady dual-porosity model, and the volume fraction of each size class associated with Building 232-F rubble.

Characteristic rubble dimension (cm)	Size range (cm)	Building 232-F volume fraction
2	$s \leq 2.8$	0.10
4	$2.8 < s \leq 5.7$	0.10
8	$5.7 < s \leq 11.3$	0.45
16	$11.3 < s \leq 22.6$	0.35
32	$22.6 < s \leq 45.3$	0
64	$45.3 < s$	0

Figures

(a)

(b)

Figure 1 Demolition of Building 232-F. (a) Felling of stack. (b) Concrete rubble.

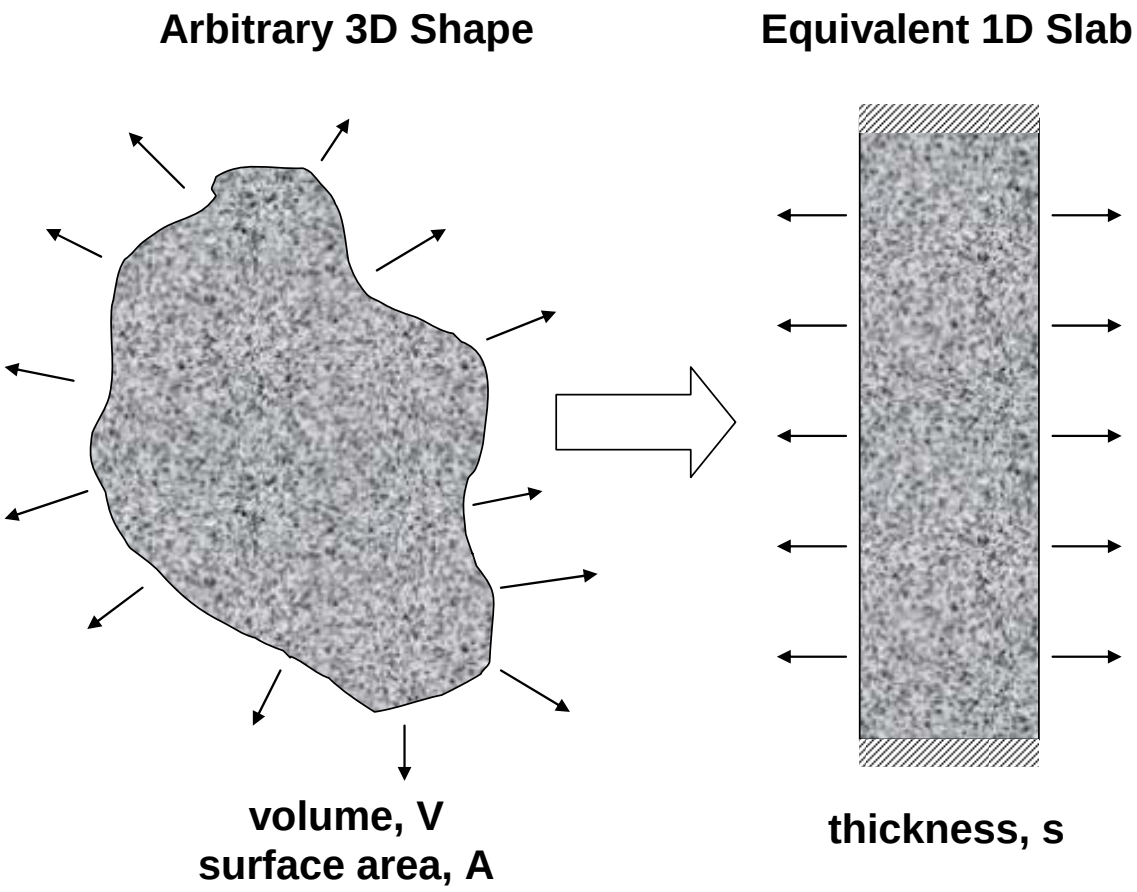

1

2 Figure 2 Three-dimensional diffusive leaching from concrete of arbitrary size and
3 shape approximated by one-dimensional diffusion from a slab.

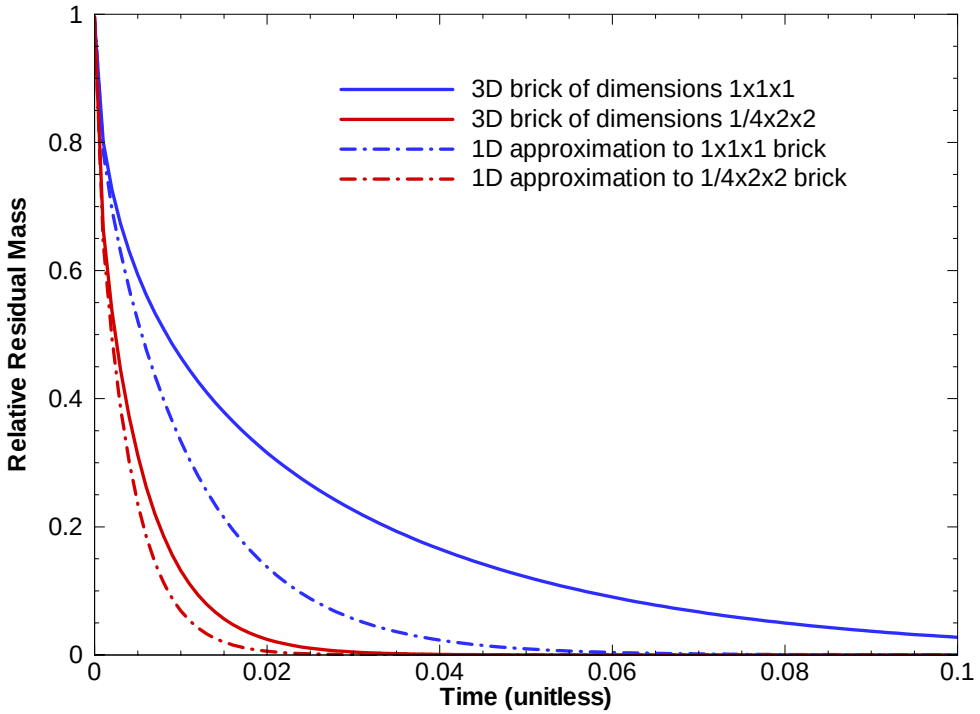

Figure 3 Relative residual mass for diffusion from three-dimensional bricks of two shapes, and corresponding one-dimensional approximations based on volume and area preservation.

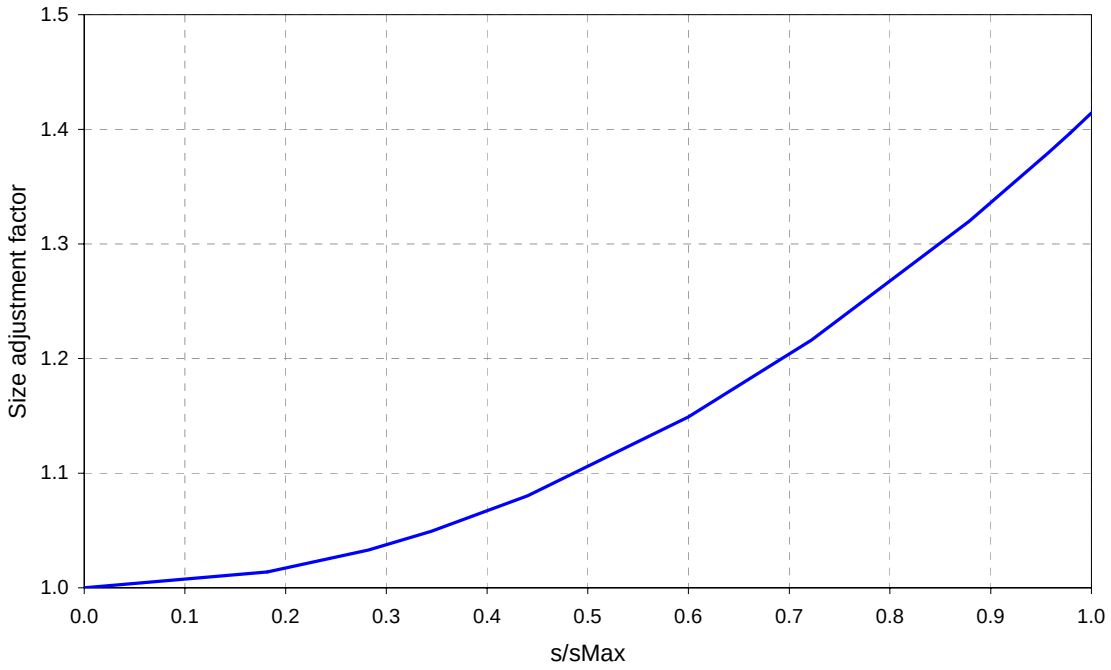

1

2 Figure 4 Empirical factor f for adjusting equivalent slab thickness s based on
3 preserving volume and surface area. Defined by equation (13).

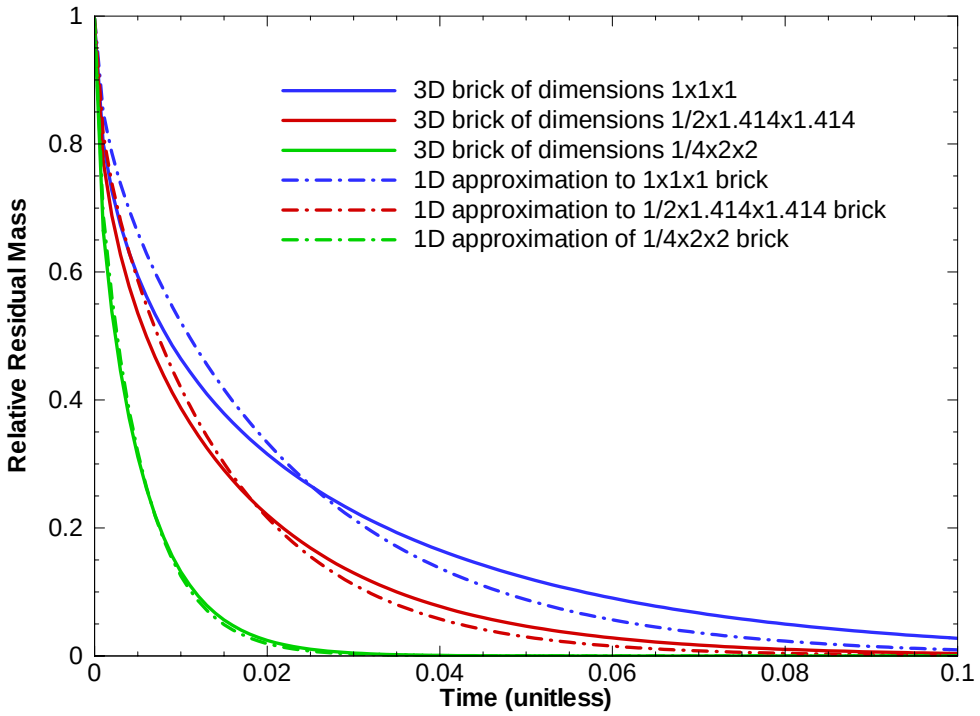

Figure 5 Relative residual mass for diffusion from three-dimensional bricks of three shapes, and corresponding one-dimensional approximations based on optimal slab thickness given by equation (14).

(a)

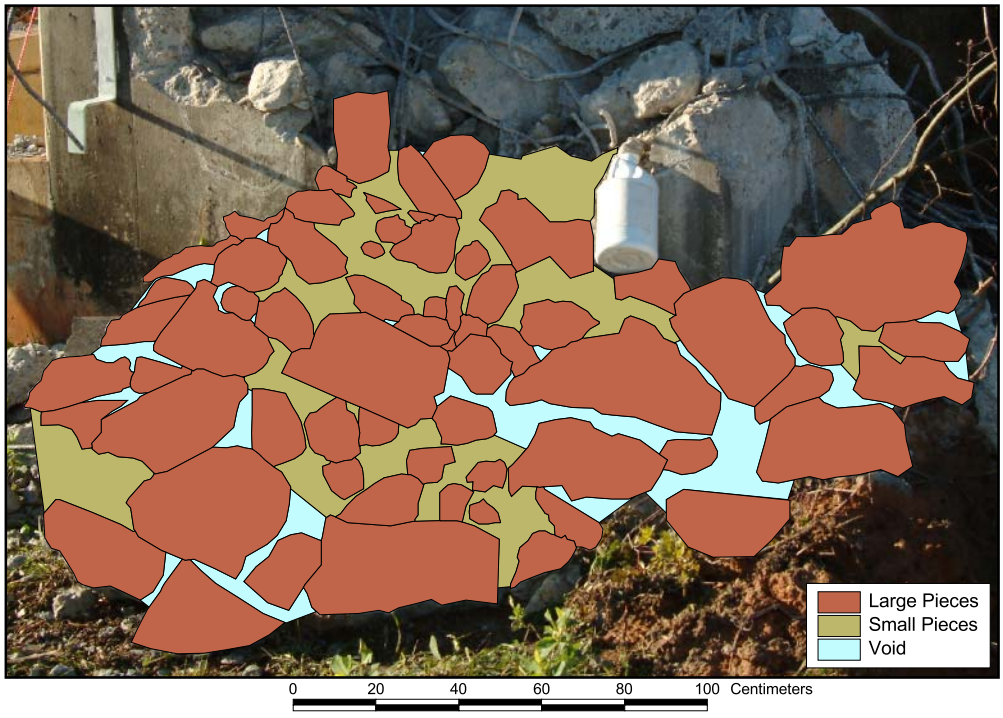

(b)

Figure 6 Concrete rubble from a demolition site comparable to Building 232-F. (a) Outlined region of interest. (b) Translation into Geographic Information System (GIS) polygons.

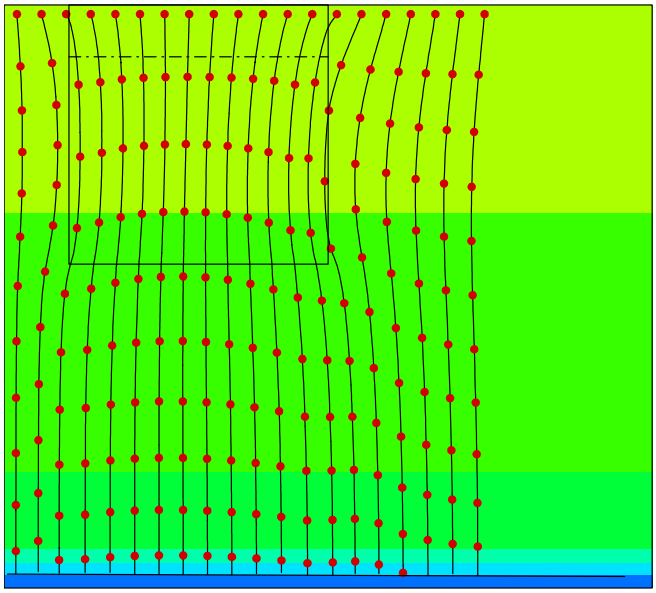

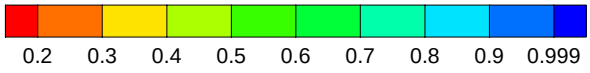

(a)

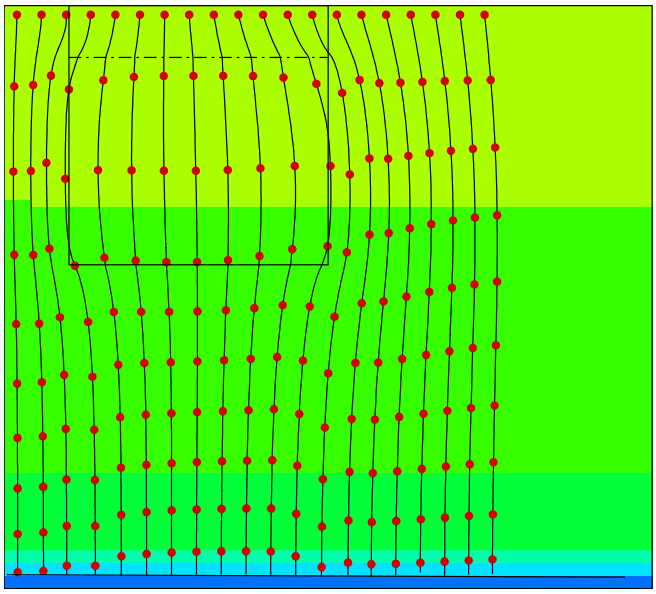

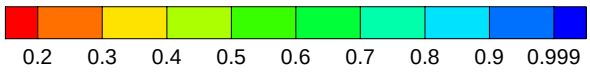

(b)

Figure 7 Simulated saturation and pathlines for disposal trenches containing (a) soil only and (b) concrete rubble backfilled with soil. One-year time markers are shown on the pathlines, which were computed from pore velocity.

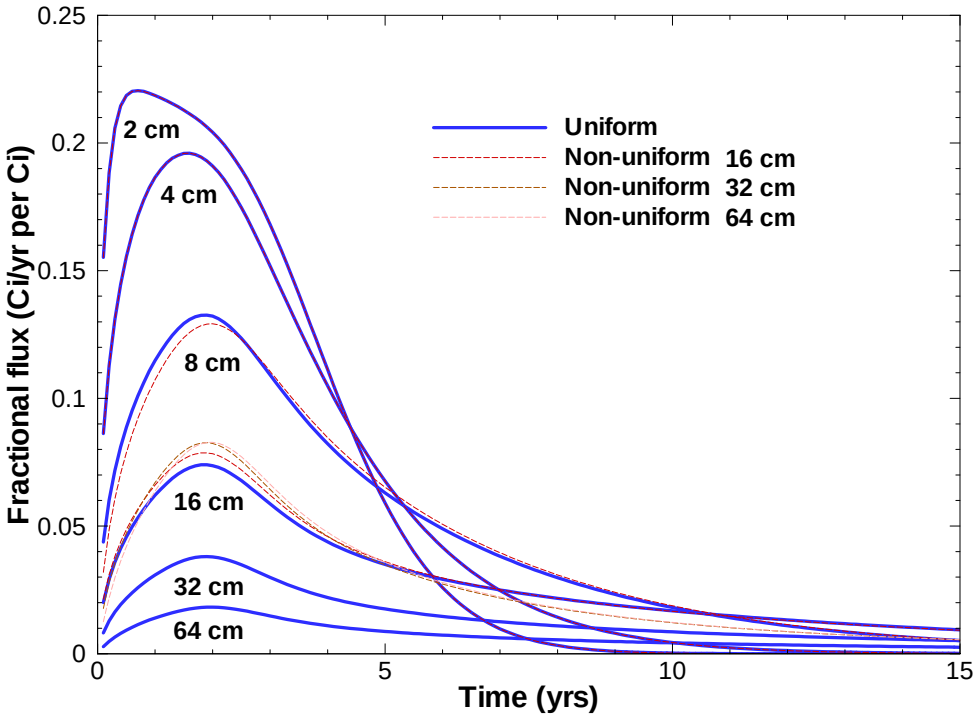

Figure 8 Simulated fractional flux of tritium released at the bottom of a disposal trench as a function of one-dimensional slab thickness and initial source distribution. Tritium is confined to the first 7.62 cm (3 inches) of depth on one side for the non-uniform initial distribution.

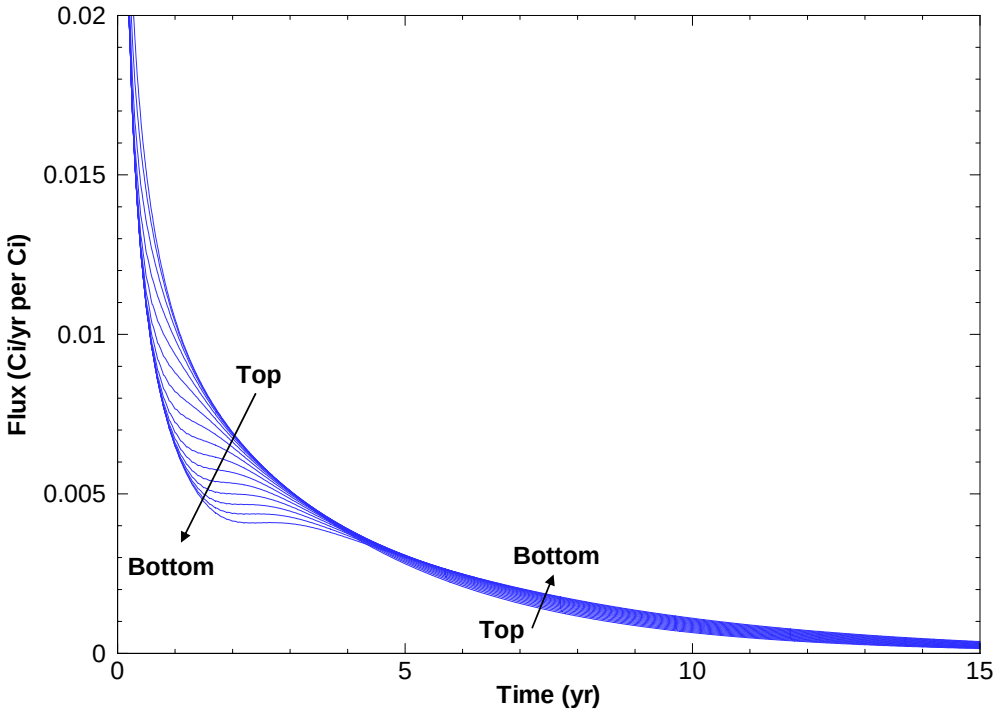

Figure 9 Fractional flux as a function of elevation in the disposal trench for an 8 cm slab thickness and uniform initial tritium distribution.

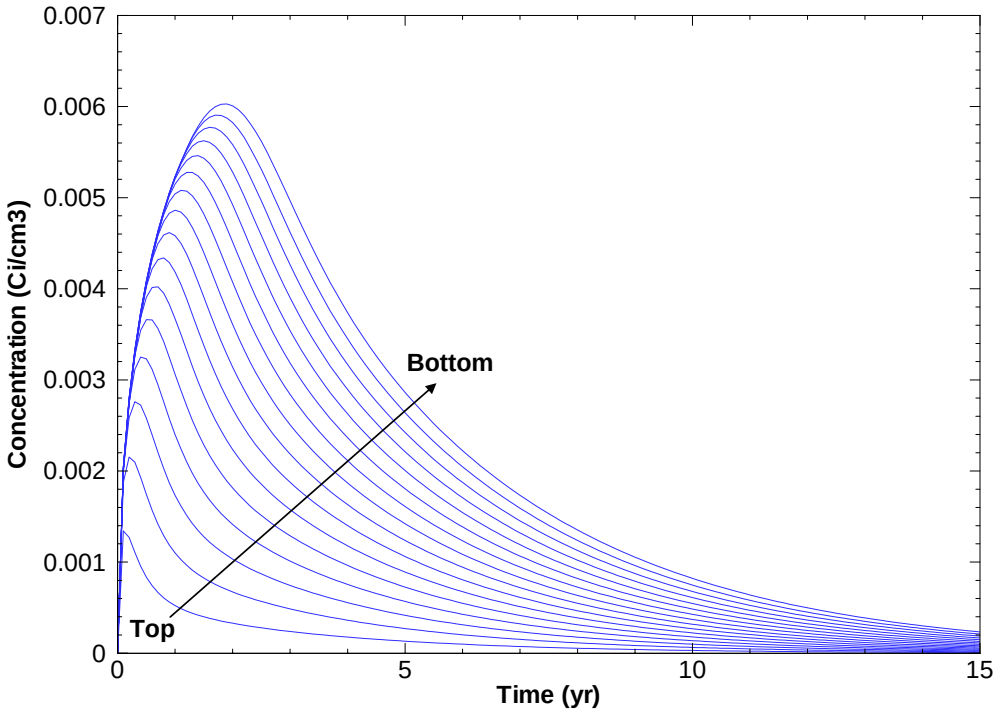

Figure 10 Soil backfill concentration as a function of elevation in the disposal trench for an 8 cm slab thickness and uniform initial tritium distribution.

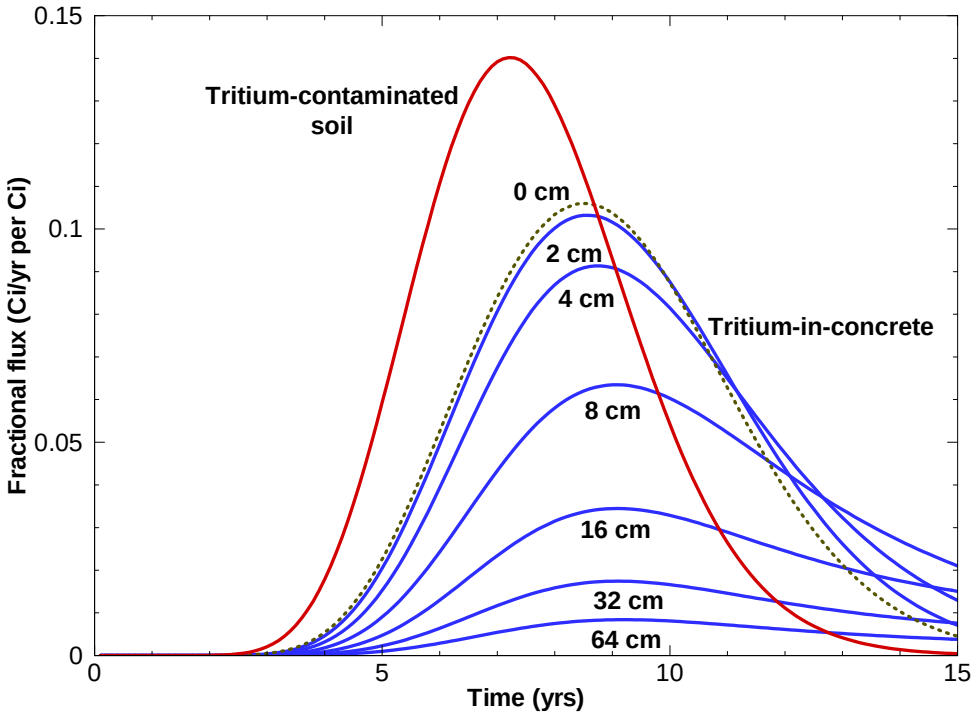

Figure 11 Simulated fractional flux to the water table from tritium-contaminated soil and concrete rubble of various characteristic one-dimensional slab dimensions.